

Wavelet Analysis of Impact Force Due to Single Bubble Shock-Induced Collapse Near Rigid and Coated Surfaces

¹Rubani Firly, ¹Kazuaki Inaba, ^{1,2}Farid Triawan, ¹Kikuo Kishimoto,

³Keisuke Hayabusa, ³Hiroaki Nakamoto

¹Department of Mechanical Engineering, Tokyo Institute of Technology, Japan

²Department of Mechanical Engineering, Sampoerna University, Indonesia

³Ebara Corporation, Japan

Abstract: The present study conducted numerical simulations of the impact force due to single bubble shock-induced collapses to discuss the failure mechanisms of the coating material in the fluid-pumps against cavitation damage. For the simplification, a bubble collapsing inside the rigid tube of 60 mm length and 1 mm radius filled with water and the impact forces were simulated and analyzed by Wavelet analysis. Near the open end of the tube, 3.75 GJ energy was placed and a shockwave was generated. The shockwave propagates into the close end, where an air bubble, 0.5 mm radius was placed and inducing it to collapse. Pressure at each gauge on the closed end were integrated to obtain the impact force. The wavelet power spectrum of the impact force was examined. At the closest stand-off distance ($\gamma=1$), wavelet transform analysis result shown that frequency of highest impact force to have a close value with theoretical bubble natural frequency. Four types of coating with acoustic impedance value of 0.9, 1.1, 13.6, and $23.2 \cdot 10^5$ (N.s/m³) (polyethylene, epoxy, aluminum, and titanium) were placed between water and rigid wall with stand-off distance $\gamma=1$. Wavelet analysis results shows dominant frequency at lower area on all materials to be close with theoretical bubble natural frequency. Higher dominant frequency on metals appear to be close with theoretical wave propagation frequency inside material, while on plastics the discrepancy is quite far.

Keywords: wavelet transform; impact force; bubble dynamics; cavitation damage.

1. Introduction

Cavitation is a formation of small vapor-filled cavities or bubble due to rapid change of pressure. Erosion is a phenomenon where surface component removed. Cavitation erosion reduces component life and performance thus brought serious maintenance issue. Hattori *et al.* [1] clarified the relation between cumulative impact energy $\sum F_i^2$ (F_i : impact load from individual bubble collapse) obtained from impact load distribution and the erosion volume loss rate. In later studies, he developed a prediction method for cavitation incubation period provided that bubble collapse impact loads are measured [2]. He also found that cumulative impact energy of cavitation jet from plastics are lower than metals, due to low acoustic impedance [3]. However, it is quite complicated to develop a relation between acoustic impedance and jet collapse impact if the parameter used is cumulative impact energy of multiple random bubbles.

Li *et al.* [4] developed Boundary Element Method (BEM) to simulate single bubble collapse and found two local high-pressure peaks near rigid wall. Another study [5] coupled BEM and FEM to observe material pit of two aluminum types on single bubble collapse. Result shown that pit was deeper and impact pressure was larger for aluminum with lower stiffness. However, they did not discuss the detail relation of impact load to material acoustic impedance.

In this study, single bubble was placed at the end of slender tube with high energy source located at the other end inducing it to collapse. At first, rigid boundary was evaluated. Then, four materials with various acoustic impedance were placed at rigid wall as coating surface. Impact loads were evaluated through wavelet analysis in order to obtain relation between jet impact and material acoustic impedance.

2. Materials and Methods

Numerical setup as shown in Fig. 1 depicts axisymmetric model of slender tube 60 mm length and 1 mm width. One tube's end remains open with transmit boundary condition while the other remain closed with rigid wall or coated materials. High energy of 3.75 GJ was placed 5 mm from open end, which will generate driving pressure of 65.6 MPa inducing an air bubble to collapse, which placed at the closed end.

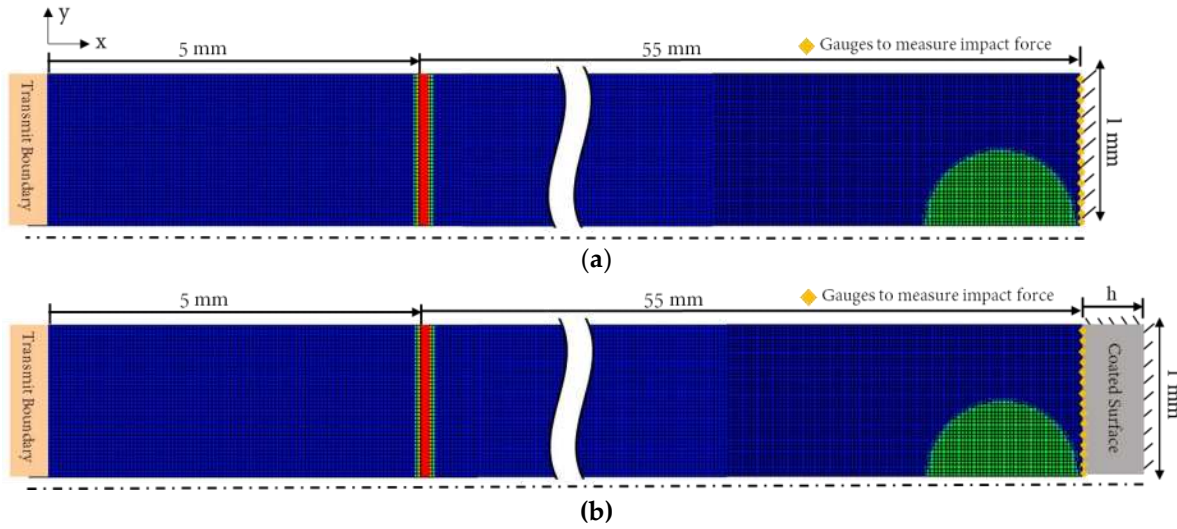


Figure 1. Numerical setup for air bubble with stand-off distance $\gamma=1$ in the vicinity of (a) rigid wall and (b) rigid wall with coated surfaces with thickness h on ANSYS AUTODYN R15.

Impact force F_w was obtained from integration of pressure value obtained from gauges installed along the wall or coated surface. Then, continuous one-dimensional Morse wavelet transform was done to analyze dominant frequency of F_w using Matlab. A preliminary evaluation of bubble natural oscillation frequency ω_n with adiabatic, liquid incompressibility, and no boundary assumption was calculated using [6]:

$$\omega_n = \left\{ \frac{1}{\rho_L R^2} \left\{ 3k(\bar{p}_\infty - p_v) + 2(3k - 1) \frac{S}{R} \right\} \right\}^{1/2} \quad (1)$$

where ρ_L is liquid density, R is bubble initial radius, k is adiabatic constant, p_v is bubble initial pressure, S is surface tension between air and water, and \bar{p}_∞ surrounding pressure. Hypothetically, bubble should oscillate in this frequency before it starts to collapse. However, due to limitation of this theory which is the absence of boundary, discrepancy between theoretical value of ω_n and frequency found in wavelet transform analysis might occur.

In order to further analyze dominant frequency of impact force on coated surface, a theoretical frequency inside material f_m was estimated based on theoretical wave propagation speed c_m . The formula is:

$$f_m = \frac{c_m}{2w} = \sqrt{\frac{E}{\rho_m}} \cdot \frac{1}{2w} \quad (2)$$

where ρ_m is coated surface density, and w is channel width which is 1 mm, rather than the coating thickness.

3. Results and discussion

3.1. Impact Force and Wavelet Analysis of Bubble Shock-Induced Collapse Near Rigid Wall

Similar numerical simulation as depicted on Fig. 1a but without bubble (shock-only case) was conducted to obtain a clear understanding on the effect of bubble’s presence to impact force on rigid wall. At 0.0305 ms in Fig. 2a, it shown that the shockwave emerged from high energy has reached the rigid wall. In Fig. 2b, the shockwave reached rigid wall at 0.0308 ms with lower impact force. This result shows that the presence of bubble could act as an obstacle which delay the time of shockwave reaching the rigid wall and also decreasing its impact force to rigid wall. At $\gamma=1$ model, highest peak of impact force occurred at 0.0331 ms which known to be originated from bubble collapse.

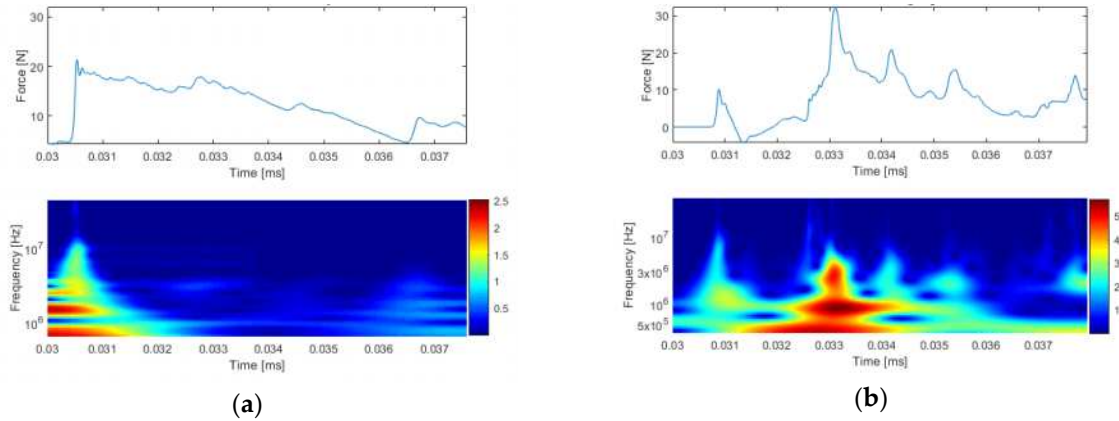


Figure 2. Wavelet transform of rigid wall for shock-only case (left), and with bubble $\gamma=1$ (right).

Bubble natural frequency was calculated using theoretical formula depicted on Eq. (1). With surrounding pressure assumed to be similar as driving pressure emerged from high energy source $\bar{p}_\infty = 65.6$ MPa, bubble natural frequency ω_n obtained was 0.887 MHz. From wavelet analysis result on Figure 2a, the dominant frequency obtained was 0.876 MHz occurred roughly at 0.032 ms to 0.034 ms. This shows that after shockwave strike the bubble, it was oscillated near its natural frequency ω_n . Discrepancy between those frequencies might occurred due to limitation of assumption used on theoretical formula (1).

3.2. Impact Force and Wavelet Analysis of Bubble Shock-Induced Collapse Near Coated Surfaces

Figure 3 shows impact force obtained on all coated surfaces along with continuous wavelet result. Theoretical wave propagation frequency inside material f_m as calculated from (2), material properties, maximum impact force F_m , its corresponding time t_m , dominant frequency obtained from continuous wavelet on high f_{Dh} and low area f_{Dl} are listed on Table 1 below. All frequency is in MHz units.

Table 1. Impact force and dominant frequency results of all material types.

Material	ρ_m (kg/m ³)	E (GPa)	Z 10 ⁵ (N.s/m ³)	f_m (MHz)	F_m (N)	t_m (ms)	f_{Dh} (MHz)	f_{Dl} (MHz)
Titanium	4510	120	23.2	1.802	22.12	0.0325	1.891	0.829
Aluminum	2700	69	13.6	2.528	23.10	0.0326	2.527	0.835
Epoxy	1186	1.03	1.1	0.466	18.89	0.0326	1.667	0.894
Polyethylene	1240	0.8	0.9	0.402	20.99	0.0325	1.677	0.893

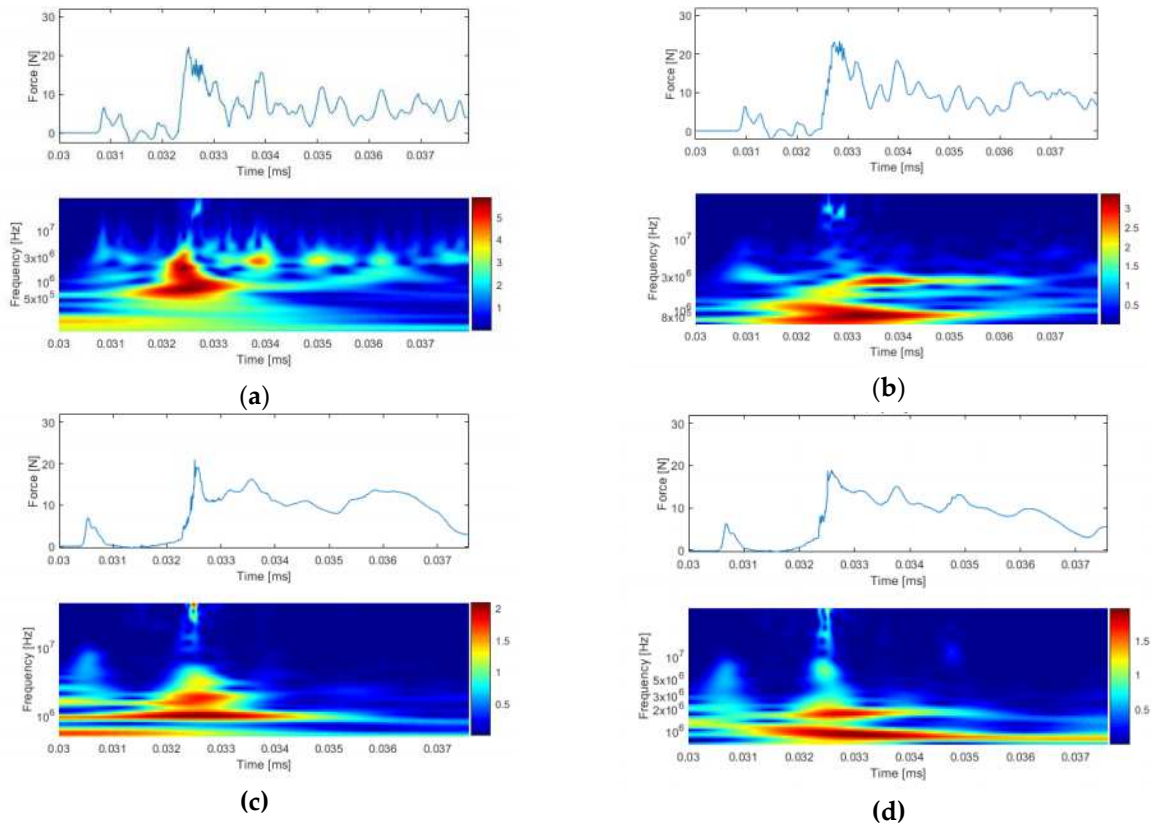


Figure 3. Wavelet transform for 5 mm thickness of (a) Titanium, (b) Aluminum, (c) Polyethylene, and (d) Epoxy.

Table 1 shows that higher dominant frequency f_{Dh} for metal materials shown to be close with theoretical wave propagation f_m whereas for plastic materials, the discrepancy is quite far. Impact force is higher on metal materials but lower on plastic materials. However, F_m of all materials is still lower from maximum impact force on rigid wall which is 32.26 N. Lower dominant frequency f_{Dl} of all materials were appeared to be close with bubble natural frequency $\omega_n = 0.887$ MHz. This show that even if coating material changes, as long as stand-off parameter γ and high energy source shockwave driving pressure \bar{p}_∞ remain constant, bubble natural frequency also remains constant. However, maximum impact force result shown that it was affected by material acoustic impedance, but since the relationship is not linear it is difficult to conclude anything. Therefore, an extensive evaluation of another mechanical property parameter should be conducted in order to establish clear relationship between impact force originated from bubble collapse.

References

1. S. Hattori, H. Mori, T. Okada, Transactions of the ASME, *Journal of Fluids Engineering* **1988**, 179-185.
2. Hattori, Shuji, Takuya Hirose, and Kenichi Sugiyama. Prediction method for cavitation erosion based on measurement of bubble collapse impact loads. *Wear* 269, no. 7-8 **2010**, 507-514.
3. Hattori, Shuji, and Takamoto Itoh. Cavitation erosion resistance of plastics. *Wear* 271, no. 7-8 **2011**, 1103-1108.
4. Li, S., Han, R., Zhang, A.M. and Wang, Q.X., Analysis of pressure field generated by a collapsing bubble. *Ocean Engineering*, 117, **2016**. pp.22-38.
5. Hsiao, C.T., Jayaprakash, A., Kapahi, A., Choi, J.K. and Chahine, G.L., Modelling of material pitting from cavitation bubble collapse. *J. Fluid Mech*, 755(9), **2014**, pp.142-175.
6. Brennen, Christopher Earls, and Christopher E. Brennen. *Fundamentals of Multiphase Flow*. Cambridge University Press, 2005; pp. 121.